Smooth nickel - a suitable anodic material in new alkaline fuel cells sulphite/oxygen

Mihaela Alexandra Lăboșel, Andreea-Floriana Enache, George-Daniel Dima, Mircea Laurențiu Dan* and Nicolae Vaszilcsin
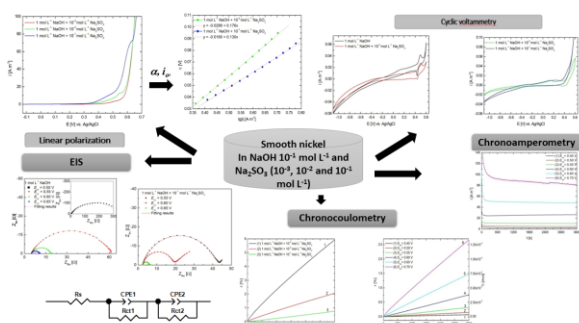
University Politehnica Timisoara, Faculty of Industrial Chemistry and Environmental Engineering, Laboratory of Electrochemistry, Corrosion and Electrochemical Engineering, 6 Pârvan, 300223 Timisoara, Romania

*to whom all correspondence should be addressed: e-mail: mircea.dan@upt.ro

Graphical abstract

Abstract

The anodic oxidation of sulphite ions was studied by voltammetric techniques on a nickel electrode in alkaline solution at various concentration of sulphite and polarization rate. The kinetic parameters of the electrode process have been determined using Tafel plots method and a mechanism of the electrochemical oxidation reaction of sulphite has been proposed. Current density, potential range of sulphite electro-oxidation and transformation degree of sulphite ions in the test solutions have been obtained by chronoamperometry and chronocoulometry. The sulphite oxidation mechanism on nickel electrode has been sustained by electrochemical impedance spectroscopy.

Keywords: Anodic sulphite oxidation, voltammetric techniques, electrochemical impedance spectroscopy, chrono-electrochemical methods, alkaline fuel cell.

1. Introduction

Sulfur dioxide, one of the most common pollutants that causes serious health and environmental problems (Yan and Wu 2017), has been investigated during the past several decades as an energy source, such as the production of hydrogen (Yan and Wu 2017; Air Quality Guidelines for particulate matter, ozone, Nitrogen Dioxide and sulfur dioxide (no date) World Health Organization; Flagiello *et al.* 2018), fuel cells (Wang and Yang. 2018; Li *et al.* 2013; Han *et al.* 2018; O'Brien *et al.* 2010), microbial cell

fuels (Huang 2013; Bouroushian 2010) and carbon dioxide reduction (Arce *et al.* 2014).

SO₂ emissions are widely converted to sulphite through the flue gas desulphurization process, in which SO₂ is scrubbed and then chemically absorbed as sulphite (SO_3^{2-}) in alkaline solutions (Flagiello *et al.* 2018). Furthermore, the oxidation of SO_3^{2-} ions can produce additional benefits, such as generation of an energy carrier like hydrogen (Han *et al.* 2018).

Sulphite electrooxidation takes place in both acidic and alkaline media, according to the reaction (1) and (2), respectively (Bouroushian 2010):

$$SO_3^{2-} + H_2O \; SO_4^{2-} + 2H^+ + 2e^- \tag{1}$$

$$SO_3^{2-} + 2HO^- \; SO_4^{2-} + H_2O + 2e^- \tag{2}$$
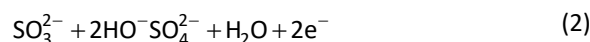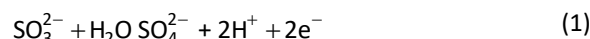
Several studies regarding the sulphite electrooxidation were performed using noble metals such as platinum (Skavas and Hemmingsen 2007) and gold (Zelinsky 2016) due to their good catalytic activity (Diaz-Abad *et al.* 2019), but the high price of these materials is a major drawback for their widespread use, therefore the present paper targets a low-cost nickel electrode.

Nickel electrodes are widely used due to the low costs and corrosion resistance in alkaline media, playing a significant role in several electrochemical systems such as rechargeable batteries (Pinkwart and Tubke 2011; Sullivan and Gaines 2012), fuel cells (McLean *et al.* 2022; Al-Saleh 1994; Schulze 2001), supercapacitors (Salleh *et al.* 2020; Xiao *et al.* 2016; Zhang *et al.* 2019), water electrolyzers (Cossar *et al.* 2019; Zayat *et al.* 2020; Seetharaman *et al.* 2014), electrochromic devices (Kotok and Kovalenko 2018; Granqvist 2015; Chen *et al.* 2020) or oxidation of organic compounds (Wala and Simka 2021; Lyalin and Petrosyan 2010). Although, over time, the electrochemical behavior of metallic nickel electrodes in different media has been intensively studied (Juodkazis *et al.* 2008), there are still doubts concerning many processes observed on the electrodes.

Most of the authors accept that in alkaline solutions metallic nickel electrode is oxidised to Ni(OH)$_2$, but some reports suggest that also NiO could be generated during the processes occurring at E< -500 mV vs. SCE (Grdeń and Klimek 2005).

The use of SO$_3^{2-}$ or SO$_2$ as an energy supply is a great challenge because of the limited researches on their oxidation catalysts (Diaz-Abad *et al.* 2019), the mechanism of the oxidation process being as well uncertain.

Therefore, further studies are still required to understand sulphite electrooxidation on metallic nickel. The present paper aims to define the kinetic parameters and the mechanism of sulphite electrooxidation on a nickel anode in alkaline solutions. The main purpose of this research is to identify the optimal conditions for recovering sulphites, thus allowing obtaining a sulphite/air alkaline fuel cell with which to produce both energy and sulfuric acid.

2. Experimental section

Electrochemical studies were performed at room temperature (25°C), in a three-electrode undivided cell connected to a Potentiostat/Galvanostat Biologics SP-150 equipped with the electrochemical impedance module. Two graphite counter electrodes were placed symmetrically to the working electrode consisting of a metallic nickel with an active surface of 0.8 cm^2 used in conjunction with a saturated Ag/AgCl reference electrode. The potential values in this paper were reported to the reference electrode (E$_{Ag/AgCl}$ = 0.197 V). The working electrode was mechanically polished with SiC grinding paper #2400 and diamond paste 3 μm, washed and ultrasonicated in distilled water for 10 minutes before every measurement in order to ensure a smooth surface.

NaOH (Merck, p.a.=99%), Na$_2$SO$_3$ (Merck, p.a.=98%) and distilled water were used to prepare NaOH 10^{-1} mol L^{-1} and different concentrations of Na$_2$SO$_3$ (10^{-3}, 10^{-2} and 10^{-1} mol L^{-1}).

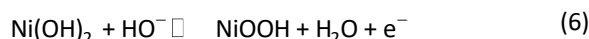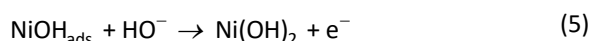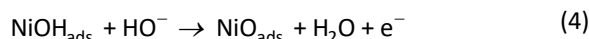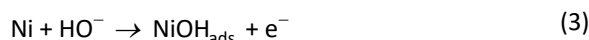Cyclic voltammograms were recorded at various scan rate (5 – 500 mV s^{-1}) and the linear polarization curves were recorded at 1 mV s^{-1}. Sulphite oxidation efficiency has been determined by chronoamperometric, and chronocoulometric methods. Electrochemical impedance spectroscopy studies were performed using the impedance module of SP-150, in the frequency range from 0.1 Hz to 100 kHz and AC voltage amplitude of 10 mV. For each spectrum, 60 points were collected, with a logarithmic distribution of 10 points per decade. The experimental EIS data were fitted to the electrical equivalent circuit by CNLS Levenberg – Marquardt procedure using ZView – Scribner Associates Inc. software.

3. Results and discussion

3.1. Cyclic voltammetry

Cyclic voltammograms have been recorded at different scan rates in order to emphasize the processes occurring at the electrode/electrolyte interface. Thus, Figure 1 presents the cyclic voltammograms recorded on nickel electrode at a polarization rate of 500 mV s^{-1}, in alkaline solutions, without and with sodium sulphite at different concentrations. To better discern and assign the voltammetric peaks and waves, the voltammograms for the solution without sulphite and for that having the highest sulphite concentration (10^{-1} M) have been drawn separately from the those for the more dilute solutions (10^{-2} and 10^{-3} M).
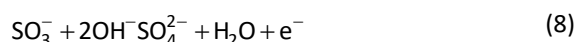
$$Ni + HO^- \rightarrow NiOH_{ads} + e^- \qquad (3)$$

$$NiOH_{ads} + HO^- \rightarrow NiO_{ads} + H_2O + e^- \qquad (4)$$

$$NiOH_{ads} + HO^- \rightarrow Ni(OH)_2 + e^- \qquad (5)$$

$$Ni(OH)_2 + HO^- \rightleftharpoons NiOOH + H_2O + e^- \qquad (6)$$

In Figure 1a, an anodic peak placed between 0.5 and 0.6 V can be distinguished in the absence of sulphite ions. It is assigned to the nickel oxidation. M. E. G. Lyons *et al.* have been shown that, initially, metallic nickel is oxidized to Ni(II) in two steps at low anodic current, following the reactions (3) and (4).
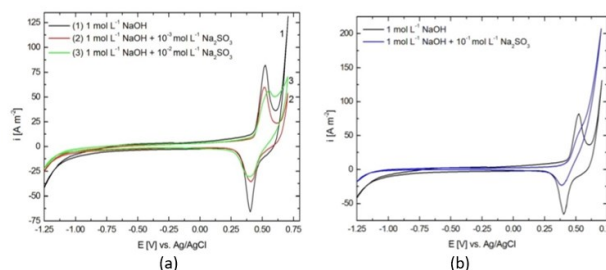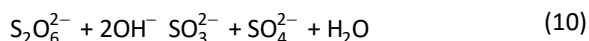

Figure 1. Cyclic voltammograms recorded on Ni electrode in 1 mol L-1 NaOH solution without and with 10-3 and 10-2 mol L-1 (a), respectively 10-1 mol L-1 (b) sulphite concentration, at 500 mV s-1

The intermediate NiOH$_{ads}$ could also participate in some other oxidation reaction as it is shown in reaction (5). Ni(II)/Ni(III) oxidation occurs during the reversible transformation Ni(OH)$_2$/NiOOH according to reaction (6), which is a final step in a complex mechanism characteristic for electrochemical behavior of nickel in alkaline media (Lyons *et al.* 2012)

In the presence of sulphite ions, the intensity of the anodic peak, corresponding to the nickel oxidation, decreases slightly because the adsorption of sulphite ions on the metal surface inhibits the anodic ionisation of nickel. On the other hand, at high concentration of sulphite (Figure 1b), a limiting current plateau coresponding to sulphite anodic oxidation, process that is mediated by Ni(OH)$_2$/NiOOH or NiOH$_{ads}$/NiO$_{ads}$ redox couple, formed on the active surface site of the nickel electrode (Enache *et al.* 2017). The electrochemical oxidation of sulphite to sulphate ions in alkaline media can be described by two possible mechanisms, the first one implies intermediate species as sulphite radical (reactions 7 and 8), and the second one the dithionate ions generation (reactions 9 and 10) (Skavas and Hemmingsen 2007):

$$SO_3^{2-} \rightleftharpoons SO_3^- + e^- \qquad (7)$$

$$SO_3^- + 2OH^- SO_4^{2-} + H_2O + e^- \qquad (8)$$

$$2SO_3^- S_2O_6^{2-} \qquad (9)$$

$$S_2O_6^{2-} + 2OH^- \; SO_3^{2-} + SO_4^{2-} + H_2O \qquad (10)$$

Simultaneously with sulphite oxidation process, oxygen evolution reaction (OER) take place, process that is controlled by charge-transfer step of the adsorbed hydroxyl species on nickel surface active site.

The peak recorded on the cathodic branch is attributed to the reduction of residual oxygen on the surface of nickel electrode or to the NiOOH reduction, the intensity of this peak decreasing with the increasing of sulphite concentration and the decreasing scan rate, as shown in Figure 2.
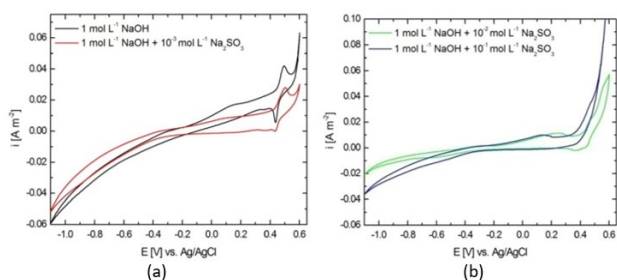
Figure 2. Cyclic voltammograms recorded on Ni electrode in 1 mol L^{-1} NaOH solution without and with 10^{-3} (a), respectively 10^{-2} and 10^{-1} mol L^{-1} (b) sulphite concentration, at 10 mV s^{-1}

3.2. Linear voltammetry

Linear voltammograms have been drawn in quasi-stationary conditions (1 mV s^{-1}) in order to identify the range potential in which only the studied process takes place. In Figure 3, the linear voltammograms obtained in the presence of different concentrations of sulphite ions are presented.
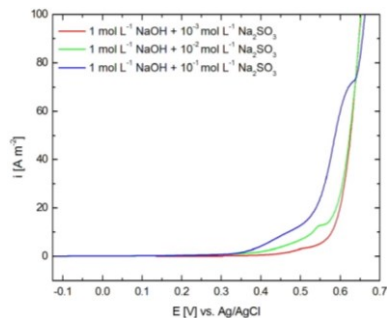
Figure 3. Linear voltammograms recorded on Ni electrode in 10^{-1} mol L^{-1}NaOH solution with different sulphite concentration, at 1 mV s^{-1}

Based on linear voltammograms, it can be seen that the sulphite oxidation waves increase with the increase of the sulphite ions concentration. A distinct and clear potential range in which the anodic process is controlled by the charge transfer can be identified only in solutions having at least 10^{-2} M sulphite.

Kinetic parameters (transfer coefficient - α and exchange current density- i_0) for electrooxidation of sulphite in alkaline solution on nickel electrode have been calculated for the two highest concentrations of sulphite, using Tafel plot method. The obtained Tafel plots are shown in Figure

4 and the calculated kinetic parameters are presented in Table 1.

E. Skavas and T. Hemmingsen have shown that for the direct oxidation of sulphite, the rate determining step is the charge transfer given by reaction (7) (Skavas and Hemmingsen 2007).

Considering that two parallel processes (direct sulphite oxidation and atomic oxygen generation) can occur in the potential range of sulphite oxidation on the electrode/electrolyte interface, the values obtained for α and i_0 are just apparent.
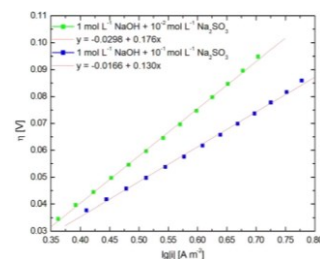
Figure 4. Tafel plot for anodic oxidation of sulphite on Ni electrode in alkaline solution with different sulphite concentration

Table 1. The kinetic parameters for sulphite oxidation in alkaline solutions

Na$_2$SO$_3$ concentration [mol L^{-1}]	b [mV dec^{-1}]	α	i_0 [A m^{-2}]
10^{-2}	176	0.34	1.19
10^{-1}	130	0.45	1.14

3.3. Chronoamperometric studies

Starting from the sulphite oxidation potential range obtained from linear voltammetry, six potential values (0.45, 0.50, 0.55, 0.60, 0.65 and 0.70 V), corresponding to the sulphite oxidation process, have been chosen in order to carry out the chronoamperometric and chronocoulometric measurements. The first four values are associated to the sulphite oxidation plateau in alkaline solutions and the last two values (0.65 and 0.70 V) corespond to the OER reaction on the electrode surface.

The obtained results for 60 minutes sulphite oxidation in alkaline solutions, at different sulphite ions concentrations, at 0.60 V, are prezented in Figure 5a. In Figure 5b, current density - time curves registered for the highest sulphite concentration are given for all six potential values at which the experiments have been carried out.
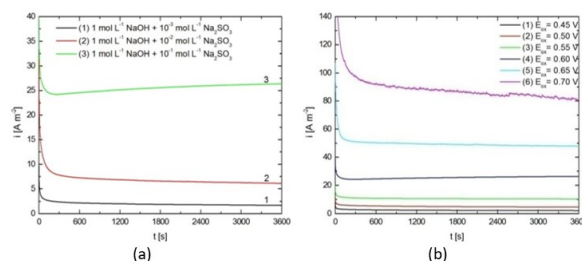
Figure 5. Current-time curves for Ni electrode in 1 mol L^{-1} NaOH solution with different sulphite concentrations, at 0.60 V (a) and in 1 mol L^{-1} NaOH + 10^{-1} mol L^{-1} Na$_2$SO$_3$ solution (b).

From chronoamperometric curves we can conclude the following aspects:

- the potential range in which sulphite anodic oxidation occurs depends on sulphite concentration, so at the lowest concentration the maximum potential for the studied process is approximately 0.50 V, while at the highest concentration the limit potential value increases at 0.60 V.

- sulphite oxidation process and OER occur simultaneously on the electrode surface at increased positive values. The shape of current-time curve recorded at E_{ox} = 0.70 V (Figure 5b) is specific for the gas evolution reaction on nickel electrode surface;

- the values of the current densities characteristic for the sulphite electrooxidation process are considerable influenced by the sulphite concentration and by the potential value at which the process is conducted;

- current density values increase with the increase of the sulphite concentration.

Based on these observations we can state that the amount of sulphite ions added to the alkaline electrolyte stimulates the first stage of OER.

3.4. Chronocoulometric studies

Chronocoulometric measurements have been performed on nickel electrode in alkaline solutions in presence of different Na_2SO_3 concentrations before and after electrochemical sulphite oxidation at maximum potential value, measuring the amount of electricity consumed for sulphite ions electrooxidation in the characteristic potential range for each Na_2SO_3 concentration added.

The variation of sulphite transformation degree during anodic oxidation as a function of time and sulphite ions concentration, when the electrochemical process is conducted at a potential value of +0.60 V, is shown in Figure 6a and 6b.
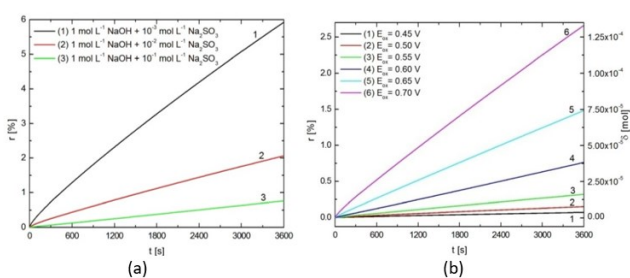
Figure 6. Chronocoulometric curves for Ni electrode in 1 mol L^{-1} NaOH solution with differenttt sulphite concentrations, at 0.6V (a) and in 1 mol L^{-1} NaOH + 10^{-1} mol L^{-1} Na$_2$SO$_3$ solution (b)

### 3.5. Electrochemical impedance spectroscopy (EIS)

In order to investigate the mechanism of oxidation for sulphite in neutral environment, the electrochemical impedance spectroscopy plots were recorded on the smooth nickel electrode in a range of Na$_2$SO$_3$ concentration before mentioned, at four potential values between +0.50 and +0.65 V. Figure 7 depicts the plotting of the Nyquist and Bode spectra, in the absence of sulphite ions (1 mol L^{-1}).
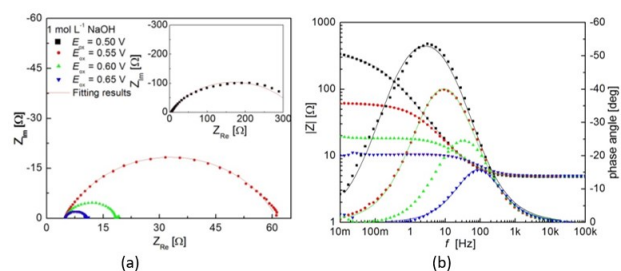
Figure 7. Nyquist (a) and Bode (b) diagrams for sulphite oxidation on nickel electrode in 1 mol L^{-1} NaOH, at different values of potential

Nyquist diagrams obtained in the absence of the sulphite ions consisted in a semicircle attributing the nickel oxidation process.

In Figure 8 and Figure 9, the Nyquist and Bode plots for different sulphite concentrarions added in the solution electrolyte support are presented.
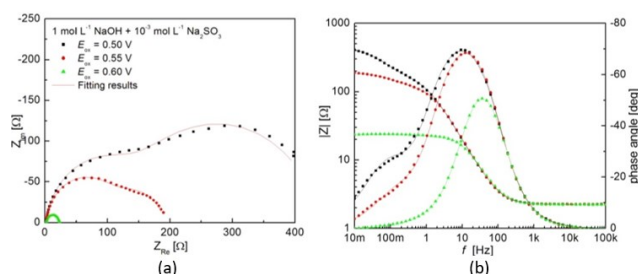

Figure 8. Nyquist (a) and Bode (b) diagrams for sulphite oxidation on nickel electrode in 1 mol L^{-1} NaOH + 10^{-3} mol L^{-1} Na$_2$SO$_3$, at different values of potential

Another semicircle attributed to sulphite oxidation on nickel electrode appears in the presence of low sulphite concentration. Both processes are controlled by charge transfer.
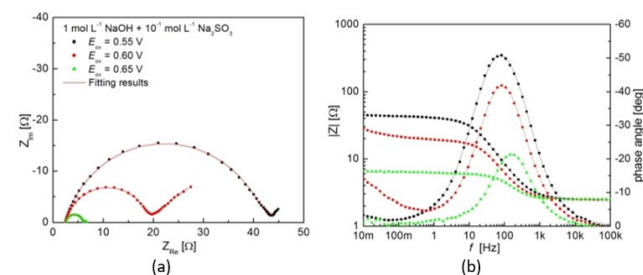
Figure 9. Nyquist (a) and Bode (b) diagrams for sulphite oxidation on nickel electrode in 1 mol L^{-1} NaOH + 10^{-1} mol L^{-1} Na$_2$SO$_3$, at different values of potential

The experimental impedance data were modeled using a complicated non-linear square technique procedure on the equivalent electrical circuit (EEC) shown in Figure 10. The resulting impedance results are graphed as continuous lines, and the corresponding values of the EEC elements are shown in Table 2.
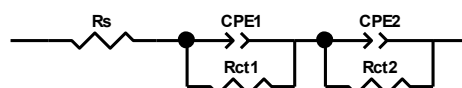
Figure 10. Equivalent electrical circuit for modeling sulphite oxidation on Ni electrode in alkaline medium.

The EEC used for analyzing impedance data for sulphite oxidation on the nickel electrode in alkaline solution consists of a resistence R_s representing the uncompensated resistance of the solution connected in series with two connections where a constant phase element (CPE) is connected in parallel with the load transfer resistance R_{ct}.

The first connection is specific to nickel oxidation, and the second is specific to sulfite oxidation process.

Analyzing the results in Table 2, it can be seen that the R_{ct} values decrease significantly with increasing sulfite concentration, indicating that the anodic oxidation of sulfite occurs at a higher rate. The values for the double layer capacitance (C_{dl}) were also calculated and it was observed that the values of this parameter increase with increasing polarization.

Table 2. Calculated impedance values for sulfite oxidation on Ni electrode in alkaline solution

Conc. Na_2SO_3 [mol L^{-1}]	E [V]	R_s [Ω cm^2]	T_1 10^2 [F cm^{-2} s^{n-1}]	n_1	R_{ct1} [Ωcm^2]	$T_2 \cdot 10^3$ [F cm^{-2} s^{n-1}]	n_2	R_{ct2} [Ωcm^2]	$C_{dl} \cdot 10_4$ [F cm^{-2}]	Chi^2 10^3
-	0.50	4.65 (0.62%)	3.41 (1.09%)	0.72 (0.42%)	329 (1.12%)	-	-	-	1.55	1.91
	0.55	4.83 (0.23%)	3.21 (0.84%)	0.74 (0.26%)	56.3 (0.32%)	-	-	-	1.52	0.62
	0.60	4.92 (0.16%)	2.34 (1.45%)	0.78 (0.34%)	13.6 (0.26%)	-	-	-	1.74	0.82
	0.65	4.97 (0.16%)	1.45 (2.34%)	0.82 (0.46%)	5.54 (0.32%)	-	-	-	1.59	0.50
10^{-3}	0.50	2.23 (0.28%)	0.97 (5.58%)	0.81 (2.08%)	309 (2.96%)	1.38 (0.93%)	0.87 (0.76%)	130.8 (3.87%)	5.83	1.03
	0.55	2.23 (0.23%)	1.72 (4.85%)	0.83 (2.90%)	86.1 (4.90%)	1.15 (0.77%)	0.91 (0.61%)	103.8 (3.20%)	6.39	0.82
	0.60	2.23 (0.16%)	2.58 (2.11%)	0.94 (1.33%)	8.14 (1.94%)	0.97 (1.08%)	0.95 (0.23%)	20.58 (0.93%)	7.07	0.88
10^{-2}	0.50	2.17 (0.28%)	0.80 (0.63%)	0.73 (2.00%)	147 (1.28%)	0.81 (1.05%)	0.86 (0.77%)	101 (3.77%)	2.89	0.51
	0.55	2.18 (0.25%)	1.08 (1.43%)	0.84 (3.23%)	48.2 (2.02%)	0.84 (1.13%)	0.93 (0.82%)	80.4 (6.08%)	4.87	0.95
	0.60	2.21 (0.16%)	1.81 (1.84%)	0.88 (3.76%)	4.04 (2.23%)	0.88 (1.12%)	0.94 (0.28%)	12.6 (1.59%)	5.98	0.78
10^{-1}	0.55	2.46 (0.22%)	0.24 (1.69%)	0.49 (5.07%)	88.4 (0.92%)	0.56 (0.89%)	0.85 (0.25%)	38.5 (0.64%)	1.77	0.14
	0.60	2.47 (0.13%)	0.33 (2.08%)	0.49 (2.81%)	31.5 (1.19%)	0.71 (0.98%)	0.87 (0.21%)	16.2 (0.44%)	2.82	0.16
	0.65	2.50 (0.22%)	0.55 (2.87%)	0.51(14.56%)	1.67 (1.55%)	0.76 (4.38%)	0.93 (0.93%)	3.39 (1.42%)	5.24	0.74

4. Conclusions

Based on the electrochemical methods applied in this study, the characteristic range of the optimal potential for each sulphite concentration added to the alkaline electrolyte solution was identified. The current densities specific for sulphite oxidation and the transformation degree as a function of the electrolysis time were also determined. The kinetic parameters (α and i_o) were calculated, showing that the general process is controlled by the charge transfer step.

It has been found that the efficiency of oxidation process is influenced by the potential value at which this process is conducted and the concentration of sulphite ions in the electrolyte. The optimum potential is 0.60V for sulphite concentrations higher than 10^{-2} mol L^{-1} added in alkaline media. We conclude that anodic sulfite oxidation occurs at a faster pace since R_{ct} values decrease with increasing sulfite content. With increasing polarization, the values of the double layer capacitance (C_{dl}) increase.

Taking into account the above conclusions, one may say that the metallic nickel electrode ought to be considered as a promising inexpensive catalyst for the electrochemical oxidation of sulphite, especially in a sulphite/air alkaline fuel cell.

References

Air Quality Guidelines for particulate matter, ozone, Nitrogen Dioxide and sulfur dioxide (no date) World Health Organization, World Health Organization, Available at: https://www.who.int/publications-detail-redirect/WHO-SDE-PHE-OEH-06-02 (Accessed: April 23, 2023).

Al-Saleh M.A., Gultekin S., Al-Zakri A.S. and Celiker H. (1994). Performance of porous nickel electrode for alkaline H_2/O_2 fuel cell, *International Journal of Hydrogen Energy*, **19**, 713–718.

Arce R., Aguirre M.J. and Romero J. (2014). Electrooxidation of Free Sulfite by an Integrated System of Glassy Carbon Modified Electrodes with Nickel Phthalocyanines and Membrane Absorber in Red Wine, *International Journal of Electrochemical Science*, **9**, 7916–7924.

Bouroushian M. (2010). Electrochemistry of Metal Chalcogenides, Springer-Verlag Berlin, Heidelberg Berlin.

Chen P.W., Te Chang C., Ko T.F., Hsu S.C., Li K.D. and Wu J.Y. (2020). Fast response of complementary electrochromic device based on WO_3/NiO electrodes, *Scientific Reports*, **10**, 1–12.

Cossar E., Barnett A.O., Seland F. and Baranova E.A. (2019). The Performance of Nickel and Nickel-Iron Catalysts Evaluated as Anodes in Anion Exchange Membrane Water Electrolysis, *Catalysts,* **9**, 814.

Diaz-Abad S., Millan M., Rodrigo M.A. and Lobato J. (2019). Review of Anodic Catalysts for SO_2 Depolarized Electrolysis for "Green Hydrogen" Production, *Catalysts*, **9**, 63.

Enache A.F, Dan M.L., Vaszilcsin N. (2017). Anodic Oxidation of Sulphite in Alkaline Media on Platinum Nanoparticles Modified Nickel Electrode, *Chemistry Journal of Moldova*, **12**, 102–109.

Enache A.F., Vaszilcsin N. and Dan M.L. (2016). Anodic Oxidation of Sulphite in Alkaline Solutions on Skeletal Nickel Electrode II, Chrono – Amperometric, Potentiometric, Coulometric and Electrochemical Impedance Studies, *Chemical Bulletin of "Politehnica" University of Timisoara, ROMANIA, Series of Chemistry and Environmental Engineering*, **61**, 58–65.

Flagiello D., Erto A., Lancia A. and Di Natale F. (2018). Experimental and modelling analysis of seawater scrubbers for sulphur dioxide removal from flue-gas, *Fuel*, **214**, 254–263.

Granqvist C.G. (2015). Electrochromic Metal Oxides: An Introduction to Materials and Devices, in: Electrochromic Materials and Devices, 1st ed., Wiley-VCH Verlag GmbH & Co, KGaA.

Grdeń M. and Klimek K. (2005). EQCM studies on oxidation of metallic nickel electrode in basic solutions, *Journal of Electroanalytical Chemistry,* **581**, 122–131.

Han J., Cheng H., Zhang L., Fu H. and Chen J. (2018). Trash to treasure: Use flue gas SO_2 to produce H_2 via a photoelectrochemical process, *Chemical Engineering Journal*, **335**, 231–235.

Huang C. (2013). Solar hydrogen production via pulse electrolysis of aqueous ammonium sulfite solution, *Solar Energy*, **91**, 394–401.

Juodkazis K., Juodkazytė J., Vilkauskaitė R. and Jasulaitienė V. (2008). Nickel surface anodic oxidation and electrocatalysis of oxygen evolution, *Journal of Solid State Electrochemistry,* **12**, 1469–1479.

Kotok V. and Kovalenko V. (2018). A study of multilayered electrochromic platings based on nickel and cobalt hydroxides, *Eastern-European Journal of Enterprise Technologies*, **91**, 29–35.

Li Y., Shang K., Lu N., Li J. and Wu Y. (2013). Oxidation of ammonium sulfite in aqueous solutions using ozone technology, *Journal of Physics: Conference Series*, **418**, 012130.

Lyalin B. V. and Petrosyan V.A. (2010). Oxidation of organic compounds on NiOOH electrode, *Russian Journal of Electrochemistry*, **46**, 1199–1214.

Lyons M.E.G., Doyle R.L., Godwin I., O'Brien M. and Russell L. (2012). Hydrous Nickel Oxide: Redox Switching and the Oxygen Evolution Reaction in Aqueous Alkaline Solution, *Journal of The Electrochemical Society*, **159**, H932–H944.

McLean G.F., Niet T., Prince-Richard S. and Djilali N. (2002). *International Journal of Hydrogen Energy*, **27**, 507–526.

O'Brien J.A., Hinkley J.T., Donne S.W., and Lindquist S.E. (2010). The electrochemical oxidation of aqueous sulfur dioxide: A critical review of work with respect to the hybrid sulfur cycle, *Electrochimica Acta*, **55**, 573–591.

Pinkwart K. and Tubke J. (2011). Fundamentals and General Aspects of Electrochemical Energy Storage, In: Handbook of Battery Materials, 2nd ed., Wiley-VCH Verlag GmbH & Co, KGaA.

Salleh N.A., Kheawhom S. and Mohamad A.A. (2020). Characterizations of nickel mesh and nickel foam current collectors for supercapacitor application, *Arabian Journal of Chemistry*, **13**, 6838–6846.

Schulze M., Gülzow E. and Steinhilber G. (2001). Activation of nickel-anodes for alkaline fuel cells, *Applied Surface Science*, **179**, 251–256.

Seetharaman S., Balaji R., Ramya K., Dhathathreyan K.S. and Velan M. (2014). Electrochemical behaviour of nickel-based electrodes for oxygen evolution reaction in alkaline water electrolysis, *Ionics (Kiel),* **20**, 713–720.

Skavas E., Hemmingsen T. (2007). Kinetics and mechanism of sulphite oxidation on a rotating platinum disc electrode in an alkaline solution, *Electrochimica Acta*, **52**, 3510–3517.

Sullivan J. L. and Gaines L. (2012). Status of life cycle inventories for batteries, *Energy Conversion and Management*, **58**, 134–148.

Wala M. and Simka W. (2021). Effect of Anode Material on Electrochemical Oxidation of Low Molecular Weight Alcohols—A Review, *Molecules,* **26**, 1–37.

Wang J., Yang P. (2018). Potential flue gas desulfurization gypsum utilization in agriculture: A comprehensive review, *Renewable and Sustainable Energy Reviews*, **82**, 1969–1978.

Xiao H., Yao S., Liu H., Qu F., Zhang X. and Wu X. (2016). NiO nanosheet assembles for supercapacitor electrode materials, *Progress in Natural Science: Materials International*, **26**, 271–275.

Yan S. and Wu G. (2017). SO_2 Emissions in China – Their Network and Hierarchical Structures, *Scientific Reports*, **7**, 46216.

Zayat B., Mitra D. and Narayanan S.R. (2020). Inexpensive and Efficient Alkaline Water Electrolyzer with Robust Steel-Based Electrodes, *Journal of the Electrochemical Society*, **167**, 114513.

Zelinsky A.G., (2016). Features of Sulfite Oxidation on Gold Anode, *Electrochimica Acta*, **188**, 727–733.

Zhang L., Shi D., Liu T., Jaroniec M. and Yu J. (2019). Nickel-based materials for supercapacitors, *Materials Today*, **25**, 35–65.